Journal of Coastal Research	16	4	1146–1150	West Palm Beach, Florida	Fall 2000

Fine-Grained Sedimentation in a Shallow Harbor

Jianhua Jiang† and Ashish J. Mehta‡

† Jainhua Jiang
ASL Environmental Sciences Inc.
1986 Mills Road
Sidney V8L 5Y3
Canada

‡ Ashish J. Mehta
Department of Civil and Coastal Engineering
University of Florida
Gainesville, FL 32611, U.S.A.

ABSTRACT

JIANG, J. and MEHTA, A.J., 2000. Fine-grained sedimentation in a shallow harbor. *Journal of Coastal Research*, 16(4), 1146–1150. West Palm Beach (Florida), ISSN 0749-0208.

Sedimentation is examined at a potential site for an oil terminal along the Aoshan channel slope in the vicinity of the East China Sea, where fine-grained sediments predominate. A feature of this slope is that due to characteristically enhanced lateral exchange of fluid momentum and suspended sediment mass, vertical profiles of flow velocity and suspended sediment concentration are more uniform than at the center of the channel. It is shown that lateral eddy diffusion at the slope is likely to be the dominant cause of this mixing. Accordingly, a two-dimensional, depth-averaged numerical model was applied to simulate historic rates of sedimentation in the study area by using an approximate method to estimate the annual rate of sedimentation, because long term data on suspended sediment were unavailable. Model-simulated rates are compared with observed patterns of sedimentation.

ADDITIONAL INDEX WORDS: *Cohesive sediments, numerical modeling, sedimentation, tidal channel, velocity profile.*

INTRODUCTION

There are numerous muddy tidal channels in the Zhoushan region of the East China Sea (Figure 1). These channels are characterized by strong tidal currents and comparatively deep waters, with depths usually greater than 30 m. They also tend to have bank slopes with an average width of ~100 m to ~500 m and maximum depths of ~20 m to ~30 m. Due to their characteristically conducive environment, such channel slopes are potential sites for constructing ports (YE and YING, 1991). Therefore, prior to construction, emphasis is naturally placed on understanding currents, resuspension, sedimentation and, consequently, bank stability. This was the case for the proposed Aoshan oil terminal in the study area.

In the ensuing presentation, typical measured profiles of tide-induced velocity and fine-grained suspended sediment concentration (SSC) in the study region are described, followed by an examination of the likely mechanism resulting in comparatively uniform velocity profiles observed on the channel slope. Then, a depth-averaged numerical model is introduced and applied to simulate historic rates of sedimentation along the slope of the Aoshan channel. Finally, the significance of the results, and conditions under which depth-averaged models may be applied for simulating bottom changes in port projects, are briefly noted.

FIELD INVESTIGATION

Aoshan channel (Figure 1) is located along the east coast of China, about 130 km south of the Yangtze River. In this region, the distribution of bottom features is uneven, with a mean water depth of about 25 m and maximum depth on the order of 50 m. The semidiurnal tide has a mean range of about 3.1 m. Bottom and suspended sediments are dominated by clayey-silts with dispersed median diameter in the range of 5.5~9.6 μm. The Yangtze River is the major source of this sediment, which is carried south towards to the study area by sustained coastal currents.

Extensive investigations of tidal currents, SSC and sedimentation near the East Headland of the Aoshan channel slope (Figure 1) were carried out during February to March, 1995 (XIA *et al.*, 1995). The survey site included the region around the future port with an area of about 1 km^2. Vertical profiles of velocity and SSC were measured at several sites within the study area and also along the center of the adjacent channel using SLC9-1 digital current meters (designed by the Institute for Marine Instruments, Qingdao) and Niskin bottles, respectively. Bottom core samples and surveys using a side-scan sonar were also obtained. An examination of sedimentation rates was carried out by means of ^{210}Pb analysis of the core samples along with comparisons of historic surveys (XIA *et al.*, 1995).

Table 1 and Figure 2 show typical vertical distributions of observed velocity and SSC. Also shown in Table 1 are data from the Tiaozhoumen channel and Daishan channel (Figure 1). Note that H is the local water depth, $\bar{U}$ is the tidal mean velocity, U_m is the tidal mean maximum velocity and $\bar{C}$ is the tide-mean SSC. It is observed that on the channel slope, unlike in the channel itself, the maximum velocity occurs at mid-depth (in two—Aoshan and Tiaozhoumen—out of three cases) rather than at the water surface. Although the vertically-averaged velocity was lower than in the channel, there

99075 received and accepted in revision 18 August 1999.

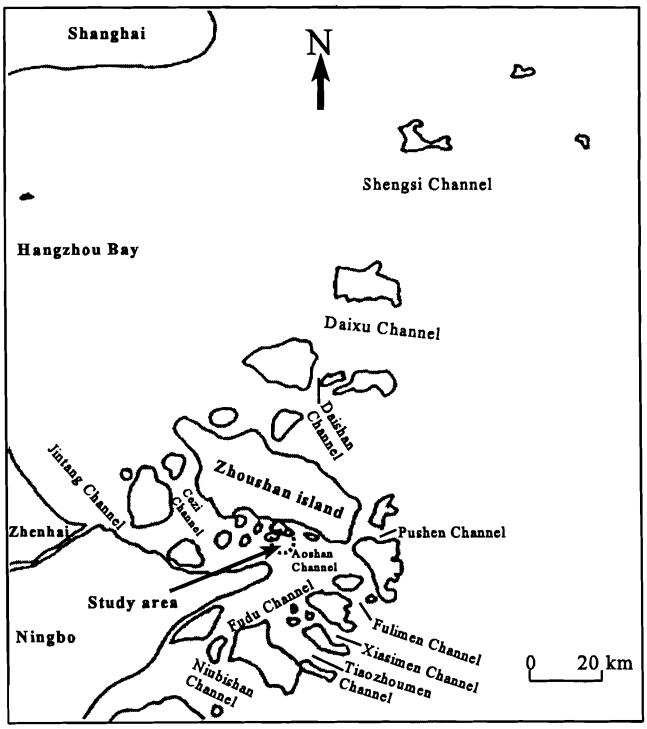

Figure 1. Location map of major channels in the Zhoushan region of the East China Sea.

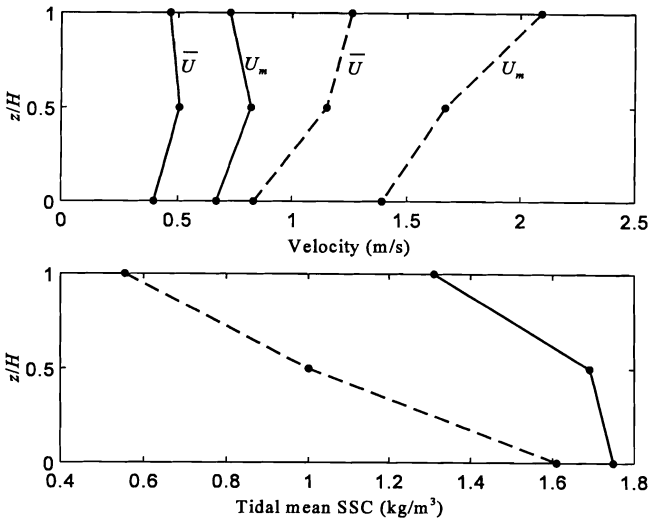

Figure 2. Typical vertical profiles of tidal velocity and SSC over the Aoshan slope (solid lines) and in the center (dashed lines).

was a comparatively strong near-bottom current on the slope with a value greater than ~40 cm/s. Since this is the typical threshold velocity of fine-grained sediment motion dominated by clayey-silts (JIANG *et al.*, 1994), this type of a velocity structure leads to a relatively low rate of sediment deposition on this slope. Table 1 and Figure 2 also indicate that, as a consequence of the velocity structure, SSC over the slope was more uniform than in the channel (in two—Aoshan and Daishan—out of three cases).

VERTICAL PROFILE OF VELOCITY

Numerous other observations have suggested that the vertical profiles of velocity on channel slopes tend to be more uniform than those found in the deeper portions of channel (FISCHER *et al.*, 1979; YE and YING, 1991; JIANG *et al.*, 1994; XIA *et al.*, 1995). However, little is known quantitatively about the precise cause of this uniformity. To evaluate this problem, one can obtain analytical solutions of the velocity profile on the slope and at the center of the channel. This purpose can be achieved by neglecting the advective terms in the flow momentum equation and assuming that both the horizontal and the vertical eddy diffusion coefficients, K_h and K_v, are constants.

The time-mean velocity, u, at any point in the channel can be assumed to have the form

$$u(y, z) = U(y)f(z) \quad (1)$$

where y is the lateral coordinate with origin at the shoreline, z is the vertical coordinate with origin at the bottom and positive upward, $U(y)$ is the vertically-averaged velocity at any point in the channel and $f(z)$ is the vertical distribution function of u. For simplicity of treatment, we will assume that $U(y)$ has a parabolic form:

Table 1. *Characteristic values of velocity and SSC observed over channel slope and in channel center during a spring tide.*

		Channel Slope				Channel Center			
Channel	Layer	H (m)	U_m (m/s)	$\bar{U}$ (m/s)	$\bar{C}$ (kg/m³)	H (m)	U_m (m/s)	$\bar{U}$ (m/s)	$\bar{C}$ (kg/m³)
Aoshan channel	surface		0.73	0.47	1.31		2.09	1.26	0.55
	middle	23	0.82	0.51	1.69	73	1.67	1.15	1.00
	bottom		0.67	0.40	1.75		1.39	0.83	1.61
Tiaozhoumen channel	surface		0.99	0.50	0.28		1.52	0.85	0.22
	middle	25	1.07	0.52	0.37	30	1.22	0.73	0.31
	bottom		0.87	0.43	0.37		0.98	0.56	0.37
Daishan channel	surface		0.84	0.52	0.50		1.48	0.77	0.36
	middle	20	0.80	0.58	1.13	35	1.39	0.75	0.57
	bottom		0.73	0.54	1.20		1.16	0.61	0.64

$$U(y) = \left[2\left(\frac{y}{l}\right) - \left(\frac{y}{l}\right)^2\right]U(l) \quad (2)$$

where l is the slope width and $U(l)$ is the velocity in the channel. Equation (2) satisfies the condition of no velocity at the bank, *i.e.,* $U(0) = 0$, channel velocity at the edge of the slope, *i.e.,* $U(y) = U(l)$, and no velocity gradient there, *i.e.,* $dU/dy = 0$ at $y = l$.

Assuming a quasi-steady state, the simplified momentum equation along the channel direction is

$$\frac{\partial}{\partial z}\left(K_v\frac{\partial u}{\partial z}\right) + \frac{\partial}{\partial y}\left(K_h\frac{\partial u}{\partial y}\right) = -gs \quad (3)$$

where g is the gravitational acceleration and s is the water surface slope along the channel. The second term on left side of Eq. (3) accounts for the lateral eddy diffusion effect. It is important over channel slope due to the large lateral gradient of velocity, but can be characteristically omitted at the channel center, where the vertical diffusion term, *i.e.,* the first term on the left hand side of Eq. (3), tends to dominate (FISCHER *et al.,* 1979). Accordingly, combining Eqs. (1), (2) and (3) along with the boundary conditions

$$f(z)\big|_{z=0} = 0, \qquad \left.\frac{\partial f(z)}{\partial z}\right|_{z=H} = 0 \quad (4)$$

the following solutions of the vertical distribution function of velocity, $f(z)$, are obtained: On the channel slope:

$$f(z) = \frac{\alpha H}{\tanh(\alpha H) - \alpha H}\left\{\frac{e^{\alpha z} + e^{\alpha(2H-z)}}{1 + e^{2\alpha H}} - 1\right\} \quad (5)$$

with $\alpha = \{(2/l^2)(K_h/K_v)[\,U(l)/U(y)]\}^{1/2}$. In the channel center:

$$f(z) = \frac{3z}{H}\left(1 - \frac{z}{2H}\right) \quad (6)$$

Figure 3 compares $f(z)$ over the slope and at the center of channel by selecting a water depth of 25 m on the slope and 40 m at the channel center. It is seen that the velocity profile on the slope is typically more uniform than in the channel center, thus demonstrating that lateral eddy diffusion can lead to a comparatively uniform velocity on the slope. It is also observed that the velocity profile on the slope is dependent on the value of α, *i.e.,* the combination of slope width, the ratio of vertically-averaged velocity in the center to that on the slope, and the ratio of turbulent momentum diffusion coefficient in horizontal direction to that in the vertical direction. For $\alpha \geq 0.3$, the velocity profile becomes almost uniform. For the three channels examined, the range of α can be shown to be 0.2–0.5, which therefore lends credence to the potential for application of a depth-averaged numerical model to simulate sedimentation.

SEDIMENTATION

Following the above observations, a depth-averaged, two-dimensional numerical model was applied to simulate historic rates of deposition and erosion. The model code consists of a hydrodynamic component and a fine-grained sediment transport component. The governing shallow water hydrodynamic equations include the vertically integrated continuity and momentum equations along with the conventional bottom and surface conditions (O'CONNOR and ZEIN, 1974; COLE and MILES, 1983).

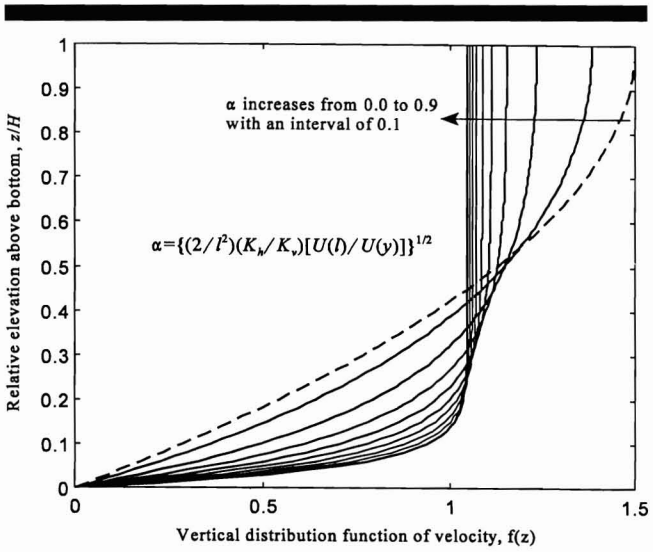

Figure 3. Analytical solutions of vertical distribution function of velocity over the channel slope (solid lines) and in the center (dashed line) for different values of α.

The vertically integrated sediment transport equation is

$$\frac{\partial HC}{\partial t} + \frac{\partial HUC}{\partial x} + \frac{\partial HVC}{\partial y} = \frac{\partial}{\partial x}\left(HD_x\frac{\partial C}{\partial x}\right) + \frac{\partial}{\partial y}\left(HD_y\frac{\partial C}{\partial y}\right) + (m_e - m_d)H \quad (7)$$

in which the fine-grained sediment deposition and erosion functions, m_d and m_e, take on the well-known forms (KRONE, 1962; KANDIAH, 1974)

$$m_d = C_b\omega_s(\tau_b/\tau_d - 1) \quad \text{for } \tau_b < \tau_d$$
$$m_e = E(\tau_b/\tau_e - 1) \quad \text{for } \tau_b > \tau_e \quad (8)$$

where x is the longitudinal coordinate, t denotes time, U and V are the vertically-averaged velocities in the x and y directions, respectively, C is the vertically-averaged SSC (omitting the overbar for convenience), D_x and D_y are the sediment mass diffusion coefficients in the x and y directions, respectively, m_d is the rate (mass per unit bed area and time) of SSC deposition, m_e is the corresponding rate of bottom sediment erosion, ω_s is the sediment (floc) settling velocity, τ_b is the bed shear stress, τ_d is the limiting shear stress for deposition, τ_e is the critical shear stress for erosion ($\tau_e = \tau_{e1}$ for newly deposited sediment and $\tau_e = \tau_{e2}$ for fully consolidated sediment), C_b is the SSC at the bed calculated from the form $C_b = \beta C$, where β (>1) is obtained by the empirical relationship of JIANG and SU (1995), and E is the erosion rate constant.

The hydrodynamic equations were solved by the Alternate Direction Implicit approach, and an Eulerian-Lagrangian scheme was adopted in the discretization of Eq. (7) (CHENG *et al.,* 1984). At the open boundaries, the M_2 harmonic component of tide and measured SSC were prescribed. Manning's

Table 2. *Selected values of important flow and sedimentary parameters.*

Parameter	Value	Parameter	Value
ω_s	3.5×10^{-4} m/s	τ_d	0.1 Pa
E	0.0005 kg/m²s	τ_{e1}	0.2 Pa
D_x, D_y	10 m²/s	τ_{e2}	0.5 Pa
β	$2.62 + 0.38 \ln(\omega_s/\kappa u_*)$	ρ_D	800 kg/m³

coefficient specifying the bottom roughness was selected to be 0.017 as a representative mean for the entire 1.1×1.0 km² area modeled. The spatial grid spacings were $\Delta x = \Delta y = 30$ m, and the time step was $\Delta t = 3$ s. The sediment transport equation was solved without flow-sediment coupling, a reasonable assumption in comparatively low SSC regimes (O'Connor and Zein, 1974; Cole and Miles, 1983).

From the model runs, the sedimentation thickness, h_f, was calculated from

$$h_f = \frac{1}{\rho_D} \sum (m_d - m_e)\Delta t \tag{9}$$

where ρ_D is the dry density of deposit. Combining Eqs. (8) and (9), one obtains

$$h_f = \frac{1}{\rho_D} \sum \left\{ C_b \omega_s \left(1 - \frac{\tau_b}{\tau_d}\right) \mathrm{H}\left(1 - \frac{\tau_b}{\tau_d}\right) + E\left(1 - \frac{\tau_b}{\tau_e}\right) \mathrm{H}\left(\frac{\tau_b}{\tau_e} - 1\right) \right\} \Delta t \tag{10}$$

where H is a unit function having the form

$$\mathrm{H}(\xi) = \begin{cases} 1 & \text{for } \xi > 0 \\ 0 & \text{for } \xi \le 0 \end{cases} \tag{11}$$

Using Eq. (10), one can evaluate the rates of sedimentation on an annual basis once the flow condition, represented by τ_b, and SSC, represented by C_b, are simulated over the entire year. However, it was not feasible to conduct these simulations because requisite observations of SSC at the open boundaries of the domain were not available. Thus, it became necessary to simplify the method of calculation. From the expressions for m_d and m_e in Eq. (8), it can be shown that the vertically-averaged SSC in the water column is approximately proportional to τ_b in areas dominated by local sedimentation. Accordingly, C_b, representing vertically-averaged SSC, can be estimated over a tidal cycle from

$$C_b = \beta C' \frac{\tau_b}{\tau_b'} \tag{12}$$

where C' and τ_b', respectively, are the simulated vertically-averaged SSC and the bottom shear stress over one tidal cycle.

Observations on the Aoshan channel slope showed that sedimentation was dominant there. Hence, the above approximate approach was adopted to predict the annual rates of sedimentation in this domain. Simulations of τ_b' and C' were initially carried out for a mean tide. Then, the hydrodynamic code was run using the measured M_2 tide, and the corresponding annual h_f was calculated at each grid-point using Eqs. (10)–(12).

Characteristic flow and sedimentary parameters required to solve Eqs. (10)–(12) were determined by means of a statistical analysis of field data, numerical modeling tests, and results from previous works (O'Connor and Zein, 1974, Nicholson and O'Connor, 1986, Mehta, 1991 and Jiang and Su, 1995). The chosen parametric values are given in Table 2, where κ (= 0.4) is the von Kármán constant, u_* is the bottom shear velocity, = $(\tau_b/\rho)^{1/2}$, and ρ is water density.

RESULTS

Observed Sedimentation

Based on historic rates of sedimentation, three regions (Figure 4 and Table 3) could be identified as follows:

(1) A region of steep slope onshore of the ~40 m depth contour with an annual mean deposition rate of ~7 cm/yr, characterized by clayey-silt with high water content, ranging from 75% to 85% by volume. The high sedimentation rate there was due to low current velocities, with a tidal mean velocity of 0–55 cm/s.

(2) A region of underwater exposed rock located mainly off the segment of the shoreline with a high cliff, without significant deposition due to shallow depths coupled with comparatively high currents, and with tidal mean velocity ranging from 60 cm/s to 80 cm/s.

(3) A region of gentle slope offshore of the ~40 m contour with late-Pleistocene deposits eroded and exposing the seabed due to high currents, with a tidal mean velocity of 55–70 cm/s.

Modeled Sedimentation

Model results (Figure 4 and Table 3) showed that the annual deposition thickness shoreward of the 40 m contour was typically 2~4 cm, and near the shoreline was generally greater than 6 cm. Also, an annual deposition thickness of 6 to 10 cm occurred in the ~15 m deep natural basin near the coast due to low velocities there. Similarly high rates of deposition also occurred in the mudflat area. No significant deposition occurred in the underwater exposed rock region. Finally, mild

Table 3. *Observed and modeled sedimentation rates over Aoshan channel slope.*

	Observed (m/yr)		Modeled (m/yr)	
Location	Range	Mean	Range	Mean
Steep slope onshore of ~40 m contour	0.033 to 0.097	0.07	0 to 0.10	0.035
Gentle slope offshore of ~40 m contour	0 to −0.026	−0.01	0 to −0.02	−0.009
Region of underwater exposed rock	0	0	0	0

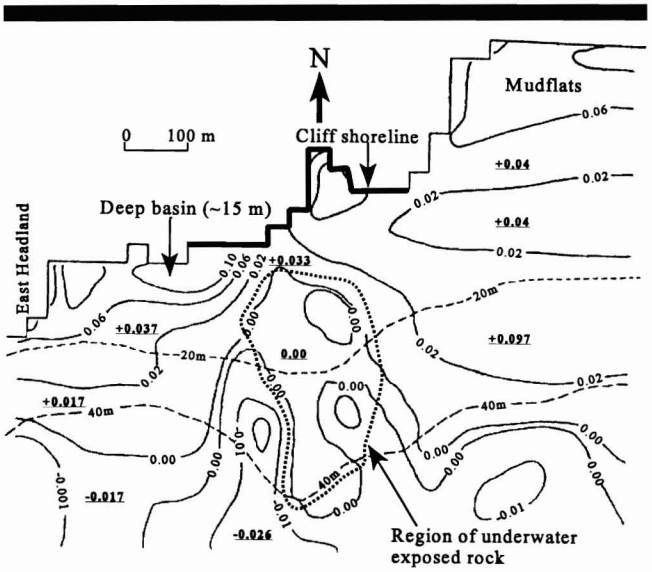

Figure 4. Contours of water depth (dashed lines) and modeled rates (m/yr) of deposition (positive) and erosion (negative). Underlined numbers are deposition and erosion rates (m/yr) obtained by topographic comparison between 1962 and 1995 surveys. Region of exposed rock is enclosed by a dotted line.

erosion was observed seaward of the ~40 m contour with an annual erosion thickness in the majority of the area less than 0.5 cm, and maximum 1 to 2 cm offshore of the East Headland.

A visual inspection of Figure 4 reveals that the above results on deposition and erosion are in general agreement with the field pattern. To further explore this observation, in Table 3 relevant ranges and corresponding means of annual rates are given for deposition (positive) and erosion (negative). In the onshore region, the modeled deposition rate range of 0 to 0.100 m/yr is somewhat lower than the measured 0.033 to 0.097 m/yr range. However, the upper limits of these range are in close agreement. Because the lower limits differ, the modeled mean deposition rate of 0.035 m/yr is one-half the observed 0.070 m/yr. In the offshore zone, the modeled erosion rates agree reasonably well with measurements.

CONCLUSIONS

The following conclusions can be drawn from this work:

1. Lateral eddy diffusion effect is believed to be the dominant mechanism causing the velocity profile to be more uniform over the channel slope than in the deeper part of channel.

2. This uniformity made it possible to use a depth-integrated numerical code for simulating sedimentation on the channel slope.

3. By calibration against field data on sedimentation, the model could be reasonably well adapted to predict the distribution of historic rates of erosion and deposition within the small harbor region, where long term observations of SSC were not available.

4. It is evident that the depth-averaging assumption can be best justified only for areas where enhanced momentum and mass exchange result in comparatively uniform velocity and SSC profiles. In the channel itself, with complex flow and sediment profile structures, a fully three-dimensional model code would clearly be more appropriate.

ACKNOWLEDGMENT

Thanks are due to Professors Xie Qinchun, Feng Yingjun, Xia Xiaoming, Li Bogen and Li Yan of the Second Institute of Oceanography, Hangzhou, China.

LITERATURE CITED

CHENG, R.T.; CASULLI, V., and MOLFORD, S.N., 1984. Eulerian-Lagrangian solution of the convection dispersion equation in natural coordinates. *Water Resources Research,* 20, 944–952.

COLE, P. and MILES G.V., 1983. Two-dimensional model of mud transport. *Journal of Hydraulic Engineering,* ASCE, 109(1), 1–12.

FISCHER, H.B.; LIST, E.J.; IMBERGER, J., and BROOKS, N.H., 1979. *Mixing in Inland and Coastal Waters.* New York, Academic, 483p.

JIANG, J.H.; XIE, Q.C., and FENG, Y.J., 1994. Investigation and assessment of the environmental conditions at future Daishan oil terminal. *Investigation Report,* Second Institute of Oceanography, Hangzhou, China, 60p. (in Chinese).

JIANG, J.H. and SU, J.L., 1995. Numerical modeling of deposition and erosion before and after construction of the tidal barrier in Yongjiang River estuary, China. *Acta Oceanologica Sinica,* 17(1), 121–129. (in Chinese).

KANDIAH, A., 1974. Fundamental Aspects of Surface Erosion of Cohesive Soils. Dissertation in Engineering, University of California at Davis, California, 236p.

KRONE, R.B., 1962. Flume studies of the transport of sediment in estuarial shoaling processes, *Final Report.* Hydraulic Engineering Laboratory, University of California, Berkeley, CA, 110p.

MEHTA, A.J., 1991. Characterization of Cohesive Soil Bed Surface Erosion, with Special Reference to the Relationship between Erosion Shear strength and Bed Density. Coastal and Oceanographic Engineering Department, University of Florida, Gainesville, FL, 83p.

NICHOLSON, J. and O'CONNOR, B.A., 1986. Cohesive sediment transport model. *Journal of Hydraulic Engineering* (ASCE), 112(7), 621–640.

O'CONNOR, B.A. and ZEIN, S., 1974. Numerical modeling of suspended sediment. *Proceedings of the 14th Conference on Coastal Engineering* (ASCE), 2, 1109–1128.

XIA, X.M.; JIANG, J.H.; XIE, Q.C., and LI, B.G., 1995. Investigation and assessment of the stability of the channel slope in Aoshan 100,000 tons oil port. *Investigation Report,* Second Institute of Oceanography, Hangzhou, China, 50p. (in Chinese).

YE, Y.C. and YING R.F., 1991. Analysis of Natural Environments and Conditions for Building Large Port in Ningbo-Zhoushan Deep Harbor Region, China East Sea. Beijing Oceanic Press, 380p. (in Chinese).